Handbook of Advanced Ceramics
S. Sōmiya *et al.* (Eds.)

5.5 Novel Colloidal Forming Technique: Direct Coagulation Casting

B. BALZER and L. J. GAUCKLER
ETH Zurich, Institute for Nonmetallic Materials, CH-8092 Zurich, Switzerland

5.5.1 INTRODUCTION

One of the most promising strategies for producing high-quality ceramics from powders is the wet-processing route. Less and smaller defects can be expected in the final microstructure due to better control of particle–particle interactions and increased homogeneity of particle packing in the wet stage compared to dry processing. Many attempts have been made in recent years to improve ceramic processing by new forming techniques. This can be achieved by either consolidating the dispersing medium or by coagulating the suspended particles. Consolidation of the dispersing medium is applied in gel-casting [1–3] where monomers in the suspension are polymerized or polymer gelation is induced at higher temperature [4]. Polymerization or gelation can be induced by UV radiation [5], by heat [6], or by a catalyst [2]. In freeze-casting and Quickset [7–10], the dispersing medium is frozen and removed after demolding by sublimation.

In flocculation and coagulation of a densely packed suspension, the interparticle forces are controlled in order to accomplish a liquid-to-solid transition. Consolidation may be induced either by applying heat, changing pH, or by increasing the ionic strength of the suspension. Bergström [11] and Napper [12] used a sterically stabilized suspension and destabilized it by heating to form a rigid green body. Lange [13], Velamakanni and Coworkers [14, 15] and Franks *et al.* [16] coagulate suspensions by adding salt and then increase the solids loading by pressure filtration or centrifugation. Pujar *et al.* [17] proposed a reaction injection molding method using heterocoagulation of silica–alumina mixtures.

Recently, we introduced a new approach based on the idea to destabilize a high solids loading aqueous suspension by a time-delayed, enzymatically catalyzed internal reaction [18–21]. The suspension, containing powder,

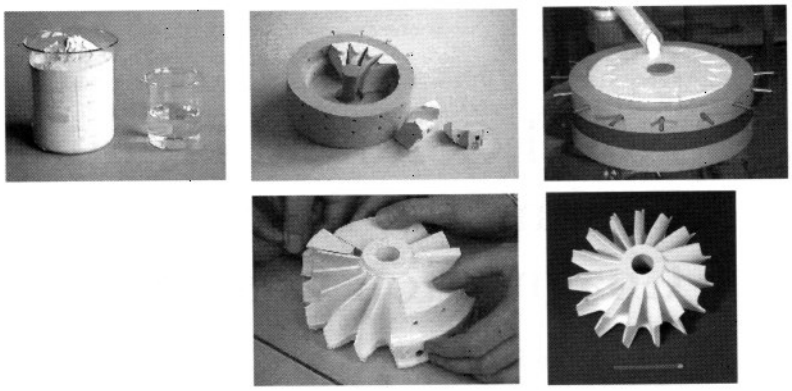

FIGURE 5.5.1 Processing complex-shaped parts by DCC: (upper row from left) starting materials, mold, casting of the suspension, (lower row from left) demolding of the wet green body, sintered turbo rotor.

a water-soluble substrate, a catalyst, and optionally polymer molecules, is cast into a mold where the products of the substrate decomposition initiate the coagulation, changing either the pH of the suspension or increasing the ionic strength. This method, called direct coagulation casting (DCC) is suitable for ceramic parts even with complex geometry (Fig. 5.5.1).

DCC combines the advantages of stabilized aqueous suspensions (cheap, harmless, and easily removable liquid; high solids content, and good flow properties) with a homogeneously induced coagulation: instead of adding the coagulating agents from outside, they are produced inside the suspension, which leads to homogeneous and strong green bodies. The coagulation rate is controlled by substrate and enzyme concentration and temperature. The amount of organics can be kept very low, therefore no special binder-removing step is necessary.

5.5.2 BASICS

In water, metal oxide surfaces are hydrolyzed:

$$MeO + H_2O \leftrightarrow Me(OH)_2$$

Depending on the pH of the liquid, the neutral particle surface will react further, forming either positive or negative surface charges [22]:

$$\text{At acidic pH:} \quad Me\text{–}OH + H_3O^+ \leftrightarrow Me\text{–}OH_2^+ + H_2O$$

$$\text{At alkaline pH:} \quad Me\text{–}OH + OH^- \leftrightarrow MeO^- + H_2O$$

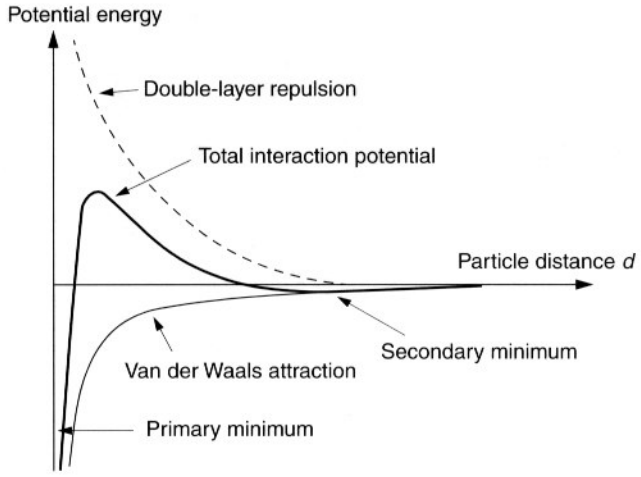

FIGURE 5.5.2 Interaction between suspended particles (electrostatic stabilization) according to DLVO theory.

When no adsorbing compounds are present, the pH therefore controls the surface charge and the surface potential Ψ_0. The pH at which the net surface charge of the suspended material is zero is called the isoelectric point (IEP). It is not a characteristic of the pure compound alone, but depends on the suspension properties as well—it can, for instance, be shifted by the presence of adsorbants that change the chemical nature of the particle surface.

According to DLVO theory [22], the net force between particles in an electrostatically stabilized suspension is the sum of the attractive Van der Waals forces and the electrostatic repulsion caused by the double layer of ions around the particle (see Figure 5.5.2).

Depending on the nature of the two contradicting forces, the resulting potential curve can show a high energy barrier preventing the particles from touching (stabilized suspension) or a barrier low enough to allow the particles to reach the primary minimum (coagulation). Furthermore, secondary minima can exist, mostly shallow ones that lead to weakly attractive forces. The double layer responsible for the electrostatic repulsion consists of the rather tightly bound Stern layer of counterions and the diffuse double layer in which counterions and co-ions diffuse freely (see Figure 5.5.3).

Within the Stern layer, the potential Ψ (V) drops linearly from Ψ_0 to Ψ_S. In the diffuse double layer, the potential decreases approximately according to:

$$\Psi = \Psi_S e^{-\kappa(d-d_S)} \tag{1}$$

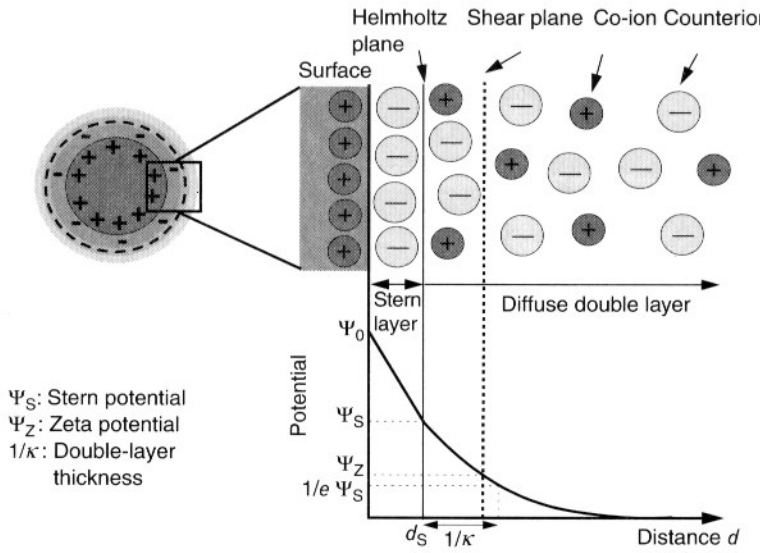

FIGURE 5.5.3 Stern model of the double layer around a positively charged particle surface (after Brinker and Scherer [22]).

Ψ_S being the Stern potential, d the distance from the particle surface, and d_S the thickness of the Stern layer. κ is the reciprocal of the double layer thickness (or Debye–Hückel length), which is defined as the distance from the Helmholtz plane at which Ψ has dropped to 1/e of Ψ_S. It is given by

$$1/\kappa = \sqrt{\frac{\varepsilon\varepsilon_0 RT}{F^2 \sum_i c_i z_i^2}} \tag{2}$$

where ε_0 (A s/V m) is the permittivity of vacuum, ε is the dielectric constant of the dispersing liquid, F (C/mol) is Faraday's constant, R (J/K mol) the gas constant, c_i (mol/l), and z_i (—) are the concentrations and valences of the ions present in the liquid. The latter add up to the ionic strength I (mol/l) of the liquid:

$$I = \frac{1}{2} \sum_i c_i z_i^2 \tag{3}$$

The higher the ionic strength, the quicker the potential drops with increasing distance from the particle surface, the thinner therefore the double layer.

In summary, the double-layer repulsion of given particles in an electrostatically stabilized suspension depends on the pH, the kind and concentration of dissolved salts, and the possible presence of adsorbing compounds. For

destabilizing the suspension, there are two possibilities: shifting the pH to the IEP (i.e. decreasing the surface potential to zero) and increasing the ionic strength (i.e. shrinking the double layer, thus reducing the range of the double-layer repulsion).

5.5.2.1 Possible Reactions For Coagulating Suspensions *In Situ*

The most obvious way to change the net potential energy curve from repulsive to attractive is to add a pH-shifting agent or a high concentration of salt. Both lead to inhomogeneous coagulation since the added compound starts to produce its effects before it could be homogeneously distributed throughout the suspension. A better way would, therefore, be to produce this agent inside the suspension by reactions that can be delayed and controlled from outside. In principle, there are two families of useful reactions for shifting the pH:

- thermally activated reactions, in particular hydrolyses, and
- enzyme-catalyzed reactions.

Some possible reactions are listed in Table 5.5.1. More information on the different agents and their effects can be found in Ref. [23].

Since nearly all of these reactions produce ions as well, they increase the ionic strength as a side-effect to the pH shift, and which of the two mechanisms leads to coagulation in the end depends mainly on the starting pH and the concentration of the agents.

We will now concentrate on the reaction that has proved most useful for coagulating aqueous alumina suspensions: the hydrolysis of urea. In principle,

TABLE 5.5.1 Possible Reaction for Shifting the pH *In Situ*

	pH shift
Thermally activated reactions	
Hydrolysis of urea ($T > 80°C$)	$3 \rightarrow 7$
Hydrolysis of formamide ($T > 60°C$)	$3 \rightarrow 7$ or $12 \rightarrow 7$
Hydrolysis of esters	$11 \rightarrow$ acidic pH, depending on pK_S of acid
Hydrolysis of lactones	$9 \rightarrow$ acidic pH, depending on pK_S of acid
Enzyme-catalyzed reactions	
Hydrolysis of urea by urease	$4 \rightarrow 9$ or $12 \rightarrow 9$
Hydrolysis of amides by amidase	$3 \rightarrow 7$ or $11 \rightarrow 7$
Hydrolysis of esters by esterase	$10 \rightarrow 5$
Oxidation of glucose by glucoseoxidase	$10 \rightarrow 4$

it can be activated thermally, but this has some drawbacks: first, the whole procedure is more difficult because the bodies will extend and have to be protected against drying; second, at higher temperature, the developing gases are less soluble in water, and instead of dissolving and influencing the pH, part of them just produce bubbles in the green body. The enzymatic catalysis, however, activates the reaction already at room temperature, and a final pH of 9 can be reached—exactly the IEP of alumina. Furthermore, urease is an enzyme readily available commercially, and by adjusting its concentration, the kinetics of the coagulation process can be controlled in a wide range.

5.5.2.2 The Urea–Urease System

The hydrolysis of urea, either at temperatures above 80°C or catalyzed by urease, leads to the formation of ammonia and carbon dioxide, which in water react further to the main products NH_4^+, HCO_3^- and a small amount of CO_3^{2-}. The buffer pH of the reaction products is around 9.2:

$$\begin{aligned} CO(NH_2)_2 + H_2O &\leftrightarrow CO_2 + 2NH_3 \\ NH_3 + H_2O &\leftrightarrow NH_4^+ + OH^- \\ CO_2 + 2H_2O &\leftrightarrow HCO_3^- + H_3O^+ \\ HCO_3^- + H_2O &\leftrightarrow CO_3^2- + H_3O^+ \end{aligned}$$

The commercially available urease is produced from jack beans and usually sold not as a pure enzyme, but in preparations containing buffers, stabilizing agents, etc. Its molar mass is given as 480 000 g/mol [24]. The effective amount of enzyme, which means the activity, is measured in units; 1 unit is defined as the amount of urease necessary to produce 1 μmol NH_3 per minute (at pH 7 and 25°C).

The urease activity depends on pH and temperature. The optimum conditions are a neutral pH and a temperature around 45°C [25], but even at room temperature a sufficient activity can be measured. Below 10°C, the enzyme works only very slowly, therefore cooling can be used to delay the beginning of the coagulation until the enzyme is added to the suspension, homogeneously distributed, and the suspension cast into molds.

5.5.2.2.1 Enzyme Kinetics

The rate of enzyme-catalyzed reactions is proportional to the enzyme concentration. At low substrate concentrations (in this case, substrate means urea),

it increases linearly with the substrate concentration, whereas above a certain high substrate concentration, it asymptotically approaches a maximum value. These observations led Michaelis and Menten to propose the following reaction mechanism [26]:

$$E + S \underset{k_{-1}}{\overset{k_1}{\rightleftarrows}} ES \xrightarrow{k_2} P + E$$

E represents the enzyme, S the substrate, ES the enzyme–substrate complex (intermediate product), P the product and k the rate constants of the respective steps.

The formation rate of the product is given by

$$r = \frac{d[P]}{dt} = \frac{k_2[E]_0[S]}{K_M + [S]} \tag{4}$$

[X] being the momentary concentration of substance X, $[E]_0$ the initial enzyme concentration and

$$K_M = \frac{k_{-1} + k_2}{k_1} \tag{5}$$

the Michaelis constant.

Equation 4 is called the Michaelis–Menten equation. $[S] \ll K_M$ gives proportionality between r and [S], whereas with $[S] \gg K_M$, the reaction rate is constant: $r_{max} = k_2[E]_0$. For urease, K_M should be between 1.4 and 30 mmol/l [25,27].

If the pH is to be shifted from around 4 to 9 in a high solids loading alumina suspension, the minimum necessary urea concentration depends mainly on the powder surface that has to be neutralized. Experiments with different urea concentrations (see Figure 5.5.4) show that, for a powder with $d_{50} = 0.5\,\mu m$

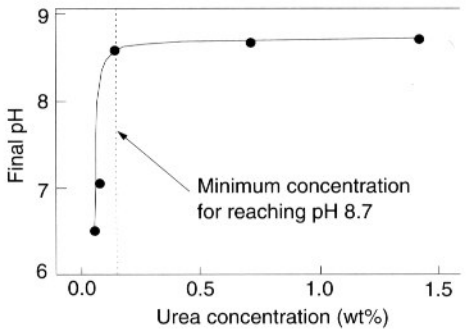

FIGURE 5.5.4 Final pH reachable with different urea concentrations in a 60 vol% alumina suspension (2 units urease per g Al_2O_3, 25°C, starting pH: 4.5).

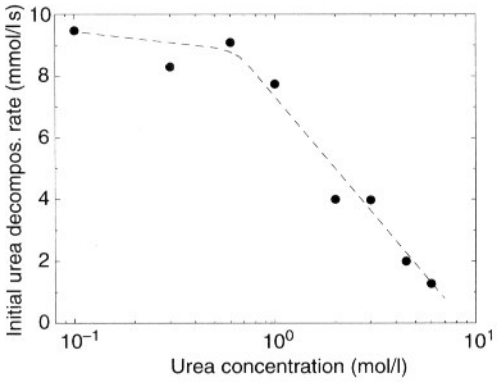

FIGURE 5.5.5 Initial urea decomposition rate (measured via conductivity) in solutions containing 30 units/ml urease and different urea concentrations (no powder!).

(BET surface 9.5 m^2/g), at least 0.17 wt% urea (based on the alumina weight) are needed to adjust a final pH of 8.7, which is sufficient to coagulate the suspension.

At low urea concentrations, the kinetics of the urea–urease system follows the Michaelis–Menten principles. If the urea concentration is too high, however (as necessary for coagulating alumina suspensions via increase of ionic strength, see Section 5.5.3.2), the Michaelis–Menten equation ceases to be valid, because urease is inhibited by urea at high concentrations, possibly because two urea molecules dock at the active sites of the enzyme where normally one urea and one water molecule should sit and react with each other [27, 28]. Figure 5.5.5 shows that this effect becomes perceptable around 1 mol/l urea.

As can be seen from the data shown in this section, the kinetics of the enzymatically catalyzed urea decomposition depends on various parameters and can be controlled within a wide range, corresponding to the respective coagulation mechanism. In the following chapters, we will show the connection between different coagulation mechanisms, their kinetics, and the resulting properties of the wet green bodies.

5.5.3 COAGULATION OF ALUMINA SUSPENSIONS BY DIFFERENT METHODS

5.5.3.1 pH SHIFT (ΔpH)

As mentioned before, alumina particles in water have an IEP of about 9. If they are stabilized around pH 4 by adding an acid, the urea decomposition can

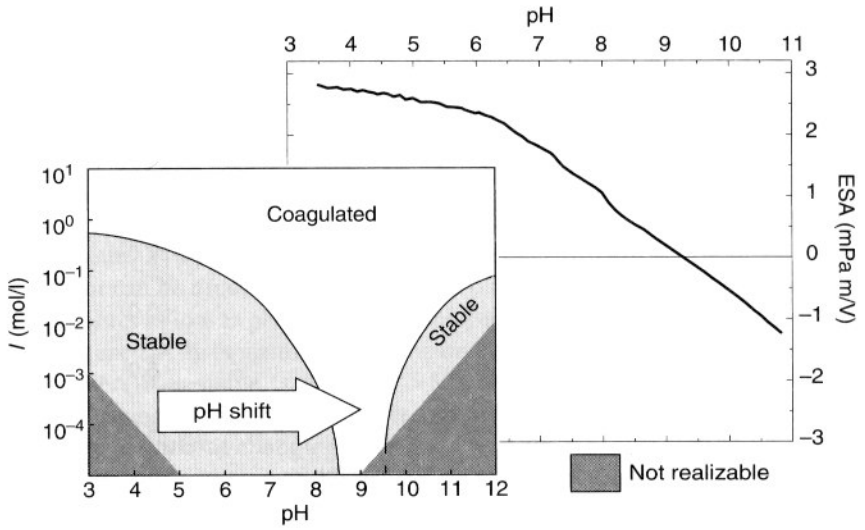

FIGURE 5.5.6 ESA (electrokinetic sonic amplitude, representing Zeta potential) signal versus pH for pure Al_2O_3 and stability diagram (schematic) of an acid-stabilized alumina suspension.

be used to shift the pH towards 9, thus reducing the repulsive double-layer potential to zero and leading to coagulation (see Figure 5.5.6). In practice, DCC samples are prepared as follows: the alumina powder is added stepwise to the water containing hydrochloric acid and urea, then the suspension is ball-milled for about 24 h and subsequently cooled with ice. The urease, dissolved in water, is added to the cooled suspension that can then be cast into the molds and allowed to warm up to room temperature where the coagulation will occur.

The experimental results given in the following were measured on suspensions or bodies made of Al_2O_3 powders with d_{50} between 0.5 and 0.6 μm.

The transition from a viscous liquid to a stiff wet green body can best be followed by oscillatory rheology. Figure 5.5.7 shows a time-dependent rheological oscillation measurement (details described in Ref. [29]) of the ΔpH coagulation of an alumina suspension. After reaching room temperature, the pH changes quickly from 4.5 to 7, whereupon the storage modulus G' and the loss modulus G'' increase sharply. In this example, the coagulation is finished within 1 h. The body starts to solidify around pH 7, and once pH 9 is reached, G' and G'' do not change any more, even though the urea decomposition may take a little more time to be completed. The change of the mechanical properties may be explained using the DLVO theory. The neutralization of the surface charge produces a deep primary minimum in the interparticle potential curves (see Figure 5.5.8). Therefore, the particles stick to each other upon first touch, and their arrangement from the stabilized suspension is practically frozen in

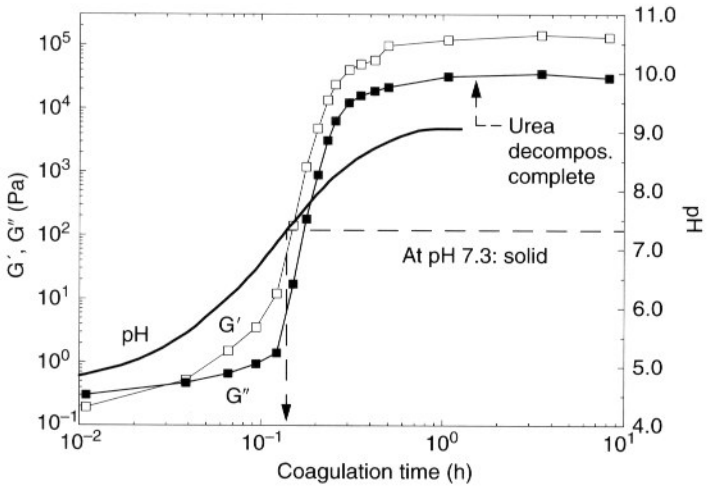

FIGURE 5.5.7 G', G'' and pH versus time for ΔpH coagulation (54 vol%, 0.2 wt% urea, room temperature).

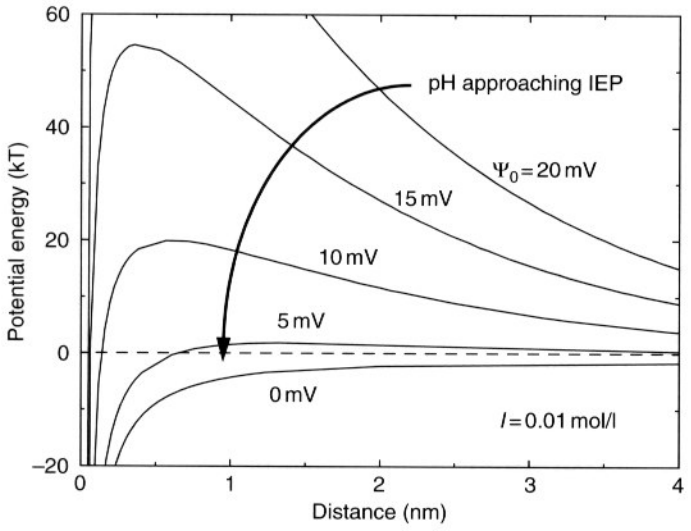

FIGURE 5.5.8 Interparticle potential energy for slurries coagulated via pH shift, calculated with Stabil 4.5 for Windows (R.V. Linhart and J.H. Adair, University of Florida, FL, USA). Hamaker Constant of alumina in water: $A = 5.32 \times 10^{-20}$ J.

(rapid coagulation), as shown by Wyss *et al.* [30]. The assumption is that this leads to a rather low medium number of nearest neighbors and a homogeneous microstructure.

5.5.3.2 Increase of Ionic Strength (ΔI)

As an example for a ΔI coagulation, an alumina suspension modified by an adsorbant can be used. Citrate ions adsorb on the alumina surface and shift the IEP to values as low as pH 3.4 for a monolayer adsorption [31]. If diammonium citrate is used as dispersant, the suspension is at the same time buffered at about pH 9 where it is stable (see Figure 5.5.9). In this case, the same enzymatic reaction as above can be used to increase the ionic strength and compress the double layer without changing the pH.

The minimum urea concentration needed for ΔI coagulation is about 1.5–2 mol/l (for pH shift, it was around 0.2 mol/l). Such high concentrations lead to inhibition of the urease as mentioned in the end of Section 5.5.2.2; therefore, somewhat higher urease concentrations are necessary, and the coagulation is still considerably prolonged. The time required to completely decompose the urea at room temperature range from some hours to more than 3 days, depending on the conditions [32].

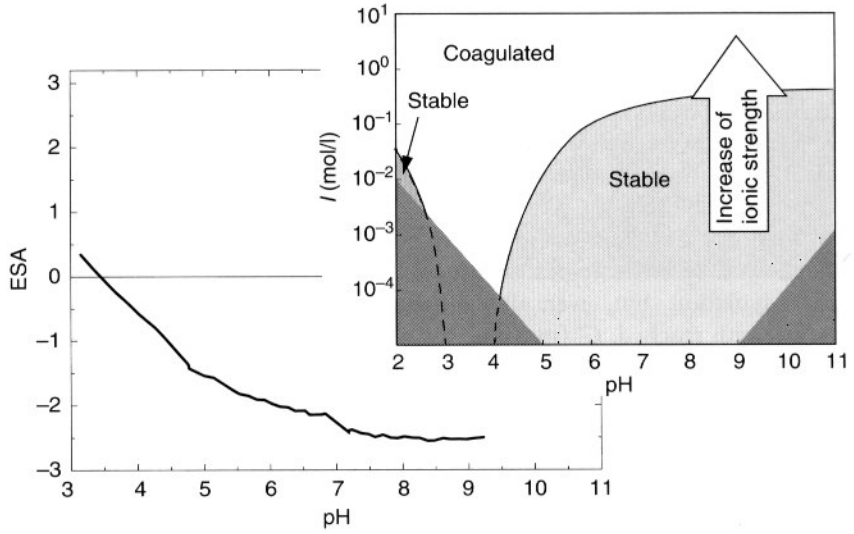

FIGURE 5.5.9 ESA (electrokinetic sonic amplitude, representing Zeta potential) signal versus pH for citrate-coated Al_2O_3 and schematic stability diagram.

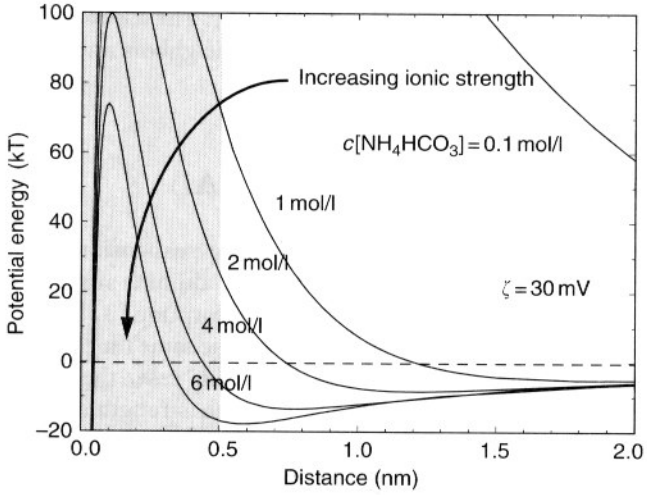

FIGURE 5.5.10 Interparticle potential energy for ΔI coagulation (grey area: 0.5-nm thick citrate layer), calculated as in Figure 5.5.8.

The increasing ionic strength leads to the development of a secondary minimum in the potential energy curves (see Figure 5.5.10). The citrate layer on the particles is about 0.5 nm thick [31], and the primary minimum lies within it; therefore, the particles cannot reach this minimum. In the shallow secondary minimum, however, the attractive forces are weak, and the particles can still move after the first touch, due to their thermal energy of about 5 kT. Thus, rearrangement can take place with time, and in the resulting network, particles have a higher average number of nearest neighbors, compared to a ΔpH network. Due to the rearrangement, shrinkage is observed in ΔI bodies, but not in ΔpH bodies [33].

In Figure 5.5.11, the coagulation of a 54 vol% alumina suspension via ΔI was followed by a rheological measurement. The process is slower than the ΔpH coagulation, but, even after all the urea is decomposed and the final ionic strength reached, G' (meaning the elastic properties) still increases with time, whereas G'' (viscous properties) decreases, indicating that rearrangement processes take place [29].

In diffusing-wave spectroscopy (DWS) measurements, the dynamics of ΔpH and ΔI systems were compared during aggregation [30]. The resulting elastic properties are in good agreement with the macroscopic rheological measurements. The DWS measurements confirm differences in microstructure between bodies produced via the two different methods: ΔI-destabilized systems are more inhomogeneous (on the length scale of a few particle

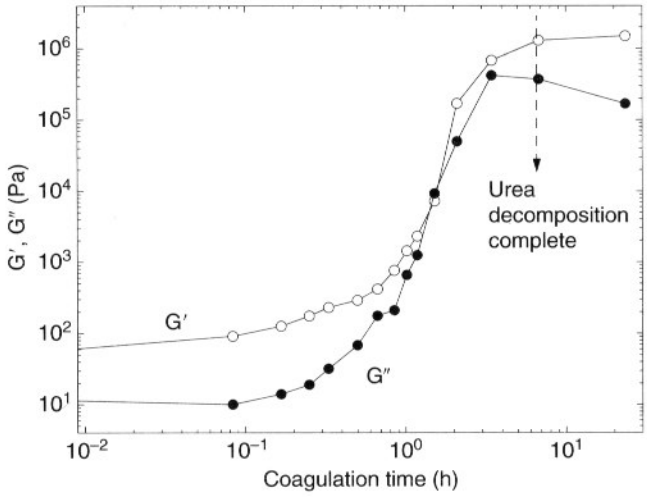

FIGURE 5.5.11 G' and G'' versus time for ΔI coagulation (54 vol%, 1.6 mol/l, room temperature).

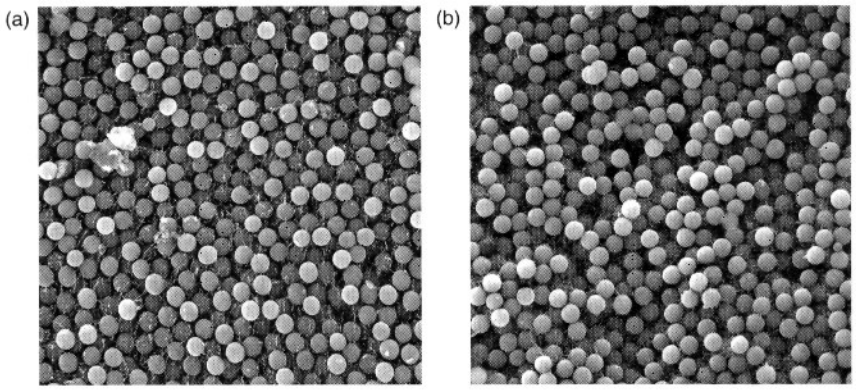

FIGURE 5.5.12 Cryo-SEM picture of (a) a stable and (b) a ΔI coagulated silica suspension (40 vol%), picture length about 10 μm [34].

diameters) than ΔpH systems. These differences can also be observed in Cryo-SEM images of high-pressure frozen (wet) samples (see Figure 5.5.12 and Ref. [34].

The consequences for the strength of the wet green bodies will be discussed in the next section.

5.5.3.3 Comparison of the Properties of ΔpH and ΔI Coagulated Wet Green Bodies

Since a freshly demolded wet green body has to withstand compression and shear forces during transport and handling even before it is dried, its strength (called "wet green strength" in the following) has to be as high as possible. The wet green strength of cylinders (see mold in Figure 5.5.13a) can be tested by compression as pictured in Figure 5.5.13b. Figure 5.5.13c shows a resulting stress–strain curve from which the wet green strength σ_c can be determined.

We have seen from the rheological measurements that ΔI coagulated suspensions need more time for solidification. In the compression tests, this becomes more evident (see Figure 5.5.14): after 2 h, ΔpH bodies have reached their final strength, whereas ΔI bodies cannot even be demolded. After 3 days, however, the ΔI bodies have obtained a strength five times higher than that of the ΔpH bodies, although their solids content is a little lower in this example.

It was already explained that in ΔpH bodies the arbitrary particle arrangement of the stable suspension is frozen in, whereas the particle network in ΔI bodies is more inhomogeneous due to the particle rearrangement during coagulation. This inhomogeneity now leads to areas of higher density.

In general, a very inhomogeneous distribution of stresses is observed for granular materials [35, 36]. A small percentage of the particles, arranged in the so-called force chains, bears the substantial part of the load. Though the length scale of these inhomogeneities in the force-distribution is longer than the length scale of structural inhomogeneities found in ΔI bodies, we assume that force chains are formed in the denser areas of the particle arrangement, where the

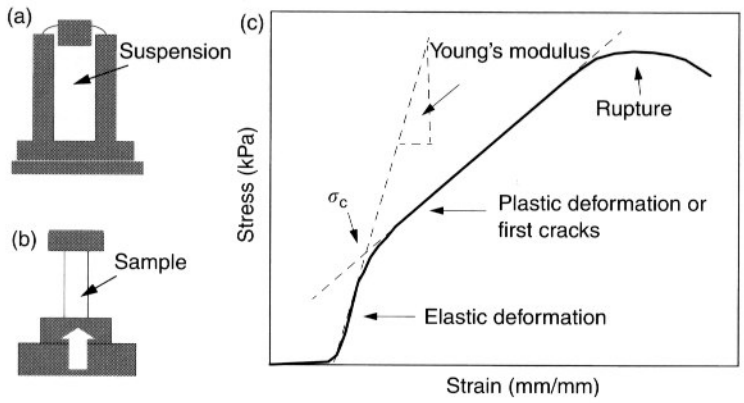

FIGURE 5.5.13 (a) Casting mold. (b) Compression test. (c) Schematic stress–strain curve.

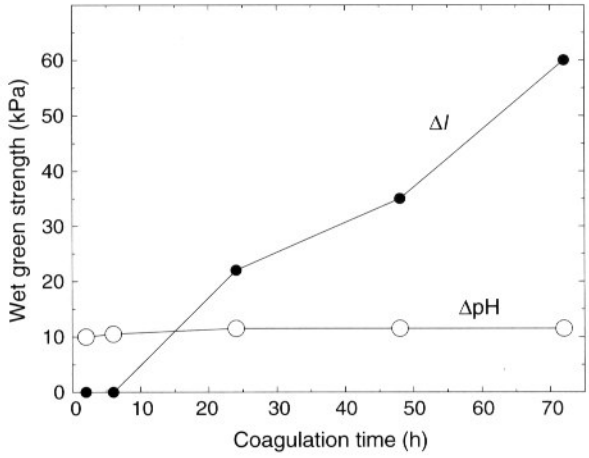

FIGURE 5.5.14 Wet green strength versus coagulation time for alumina cylinders coagulated via ΔpH (59 vol%) and ΔI (58 vol%).

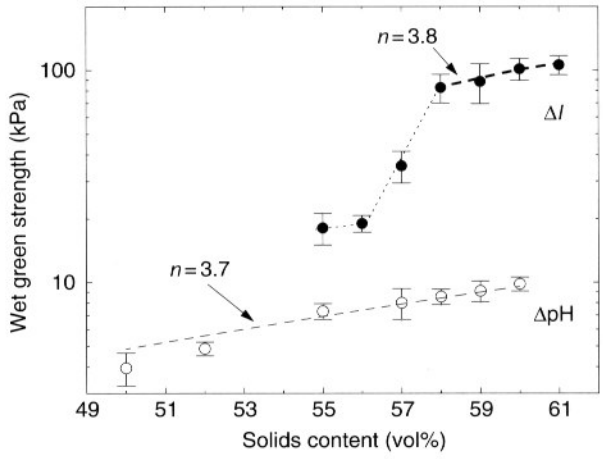

FIGURE 5.5.15 Wet green strength versus solids content for alumina cylinders coagulated via pH shift and increase of ionic strength (coagulation time: 3 days).

coordination number is higher. Consequently, structural inhomogeneities as observed in ΔI bodies would increase the mechanical strength of the particle network.

If the strength values for different solids contents (Figure 5.5.15) are compared, we see that even the dependence of the wet green strength σ on the solids content Φ is different for the two coagulation methods. The ΔpH data

can be fitted by a power law derived from percolation theory, as, for instance, used by Yanez *et al.* [37]:

$$\sigma \propto (\Phi - \Phi_c)^n \tag{6}$$

where Φ_c is the percolation threshold (here: $\Phi_c = 0.16$, after Zallen [38]). n was found to be 3.7, which corresponds well with the exponents between 3 and 5 usually given for similar systems [39, 40]. For ΔI, the strength values at $\Phi = 58$ vol% and above obey the same law with $n = 3.8$, but below, there is a shift to another dependency, which is yet to be investigated further. One could assume that, in a ΔI sample at solids loadings below 58 vol%, the particle density is too low to form dense force chains that are still able to construct a strong network throughout the whole body; therefore, the wet green strength drops to values relatively near those of the ΔpH body.

5.5.4 DCC OF PARTICLE SYSTEMS WITH POLYMER BINDERS

Polymer binders are used in ceramic forming to increase the strength of the green bodies. This effect can be exploited in DCC for increasing the wet green body strength as well. If binders are to be used in DCC they have to meet three basic requirements:

1 the addition of the binder must not increase the suspension viscosity substantially;
2 the binder has to react to a change in pH or ionic strength;
3 the swelling, gelling, etc., of the binder has to occur time-delayed, otherwise its coagulation would be quicker than that of the powder.

A class of substances fulfilling all these requirements are polyelectrolytes on the basis of polyacrylic acid. As an example, we will present the use and effects of alkali-soluble swellable thickeners (ASTs), in this case two commercially available thickeners, Acusol 820 and 830 (more details in Ref. [41]).

ASTs are cross-linked copolymers consisting of hydrophobic (e.g. ethylene, butadiene, styrene) and hydrophilic monomers (carbonic acids as acrylic, methacrylic, fumaric or maleinic acid). At low pH, the carboxyl groups are undissociated, which, together with the hydrophobic components, makes the polymer insoluble. At high pH, the carboxyl groups deprotonate, the now negatively charged groups repel each other, their hydratization improves, together resulting in the polymer particle growing and taking up water, that is, swelling (see Figure 5.5.16).

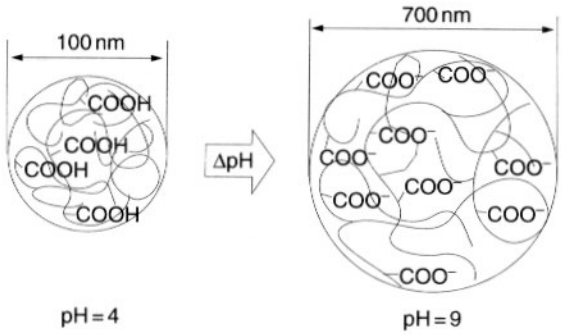

FIGURE 5.5.16 Swelling of AST molecules upon the transition acidic (insoluble) to alkaline (deprotonated, soluble).

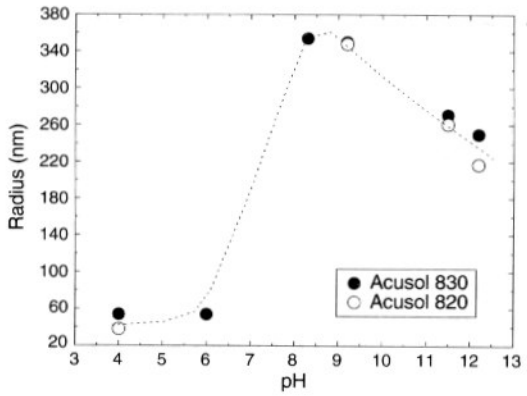

FIGURE 5.5.17 Radius of Acusol molecules in dependence of pH, measured by light scattering (data from Ref. [41]).

Figure 5.5.17 shows how the radius of Acusol particles changes with pH. The fact that the maximum size (seven times the original radius!) is reached just around pH 9 makes Acusol an excellent binder for the coagulation of alumina via DCC (ΔpH).

On the other hand, the negative charges are screened by counterions dissolved in the solution; therefore, a high ionic strength reduces the diameter of the swollen polymer "spheres", which makes Acusol unsuitable as binder for the ΔI coagulation, also because the starting pH of 9 is in the wrong region as well.

For increasing the green strength of wet alumina bodies in the DCC process, only very small amounts of ASTs are necessary (see Figure 5.5.18, the polymer amount is calculated based on the alumina weight). Whereas binderless samples

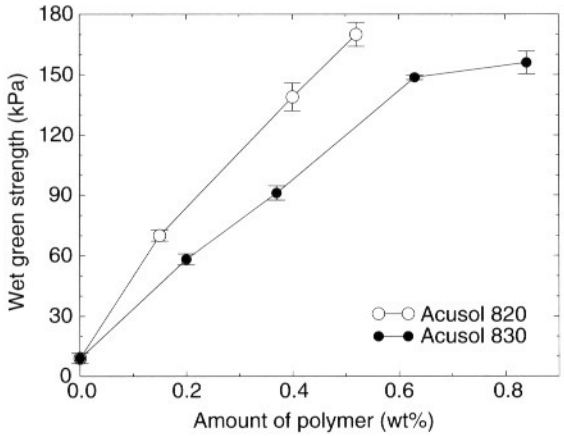

FIGURE 5.5.18 Wet green strength of Al_2O_3 bodies (ΔpH, 57 vol%) with different Acusol contents (data from Ref. [41]).

reach strength values around 10 kPa, up to 170 kPa can be found with Acusol addition. The maximum possible polymer content is found around 0.5–1 wt% since too many swelling polymer particles can induce cracks in the powder network. In addition, too strong a swelling makes the body volume increase, thus the bodies cannot be demolded.

Our explanation for this extraordinary increase in strength caused by Acusol is just an assumption that could not be proven yet. The experimental results [41] suggest that, first, the strength added by the polymer gel is far too small to add significantly to the strength of the particle network. Second, there is no perceptible bridging involved. On the other hand, the swelling of the polymer particles seems to be the crucial factor in the strengthening effect. The swelling polymer cannot fill every small water "isle" between the alumina particles, but it can try to suck the water out of it. This could draw the particles closer together, decreasing the surface-to-surface distance that increases, on the one hand, the local solids loading and, on the other hand, the bond strength between the particles.

5.5.5 OTHER CERAMIC MATERIALS

Of course, the DCC method is not restricted to alumina only. Two other ceramic compounds that were already coagulated via DCC shall be mentioned here as examples: SiC and Si_3N_4. Silicon carbide (IEP around 2–3), with boron and carbon black as sintering additives, could be stabilized at pH 11 using

tetramethyl ammonium hydroxide (TMAH) and coagulated by increasing the ionic strength with the urea/urease system [42, 43]. Wet green strength values up to 50 kPa could be achieved depending on urease concentration and coagulation time.

A mixture of α-Si_3N_4 with Al_2O_3 and Y_2O_3 as sintering aids can be coagulated via DCC as well, though the processing is more complicated [44]. Since the IEPs of the three powders are very different, all the surfaces have to be modified in order to process them together. This can be done with citric acid for the two oxides and with $Al(OH)_3$ for Si_3N_4. Afterwards, the pH is adjusted around 9.5 with TMAH, and the ionic strength is increased as above, giving wet green bodies with strength values up to 200 kPa (58 vol%) that can be sintered to 97% of the theoretical density.

5.5.6 SUMMARY AND OUTLOOK

The DCC method allows to control the interparticle forces in a suspension via an internal chemical reaction. It can be used for producing ceramic components with complicated shapes (see Figure 5.5.19), homogeneous microstructures, high strength, and reliability [45]. This ceramic forming technique might also find applications in microfabrication of very small ceramic components and structures used for sensors and actuators. Small ceramic dots, lines, and three-dimensional objects made from ceramic suspensions may become useful in MEMS technology (see Figure 5.5.20).

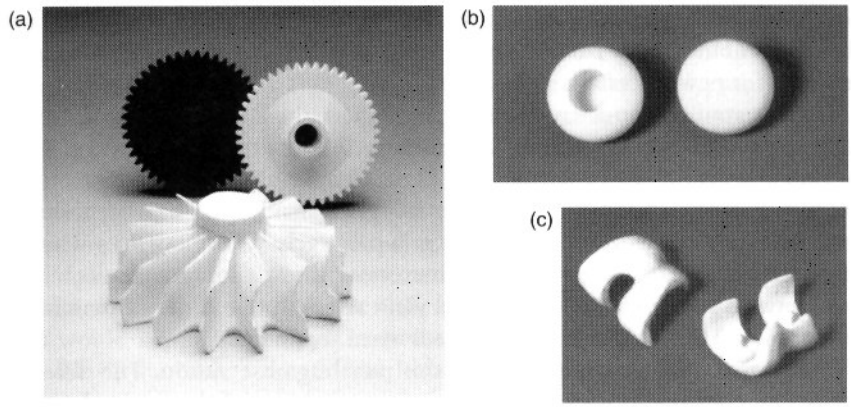

FIGURE 5.5.19 Ceramic parts produced via DCC: (a) SiC and Al_2O_3 cog-wheels and Al_2O_3 turbo rotor; (b) Al_2O_3 hip joint spheres; (c) Al_2O_3 knee implants.

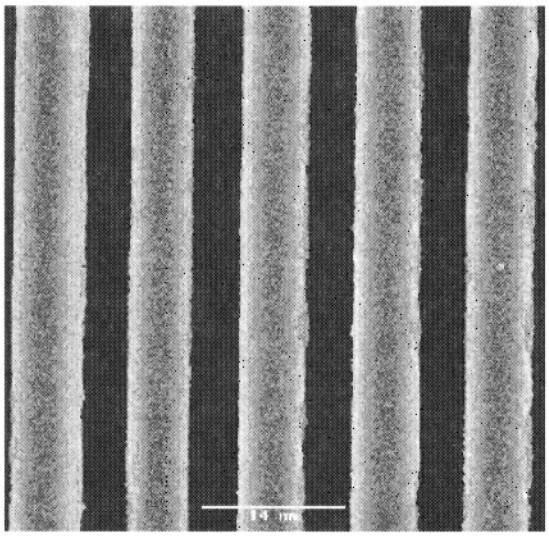

FIGURE 5.5.20 Alumina lines (7 μm in thickness) on a Si substrate, from Schönholzer *et al.* [52].

Besides triggering the sol–gel transition of electrostatically stabilized suspensions, DCC can also be used to change the conformation of polymers in suspensions and thereby change the mechanical properties from a viscous liquid to a viscoelastic gel. Examples are ASTs [41], polysaccharides, and alginates [46]. Another class are polymer emulsions containing two oligomers, one in the hydrophilic phase and the other in the hydrophobic phase. Upon changing the pH by an internal reaction, both react forming a three-dimensional cross-linked polymer network in the aqueous phase [47]. These polymers can also be combined with particle suspensions in order to create new processing methods for new materials.

Besides application-oriented topics, a method like DCC can offer new possibilities to solve basic scientific questions that are still open today. The mechanical properties of particle gel networks are highly dependent on the chemical pathway used to induce the sol–gel transition. It has been shown earlier that changing the pH produces comparatively weak networks whereas destabilizing a particle suspension via increasing the salt content results in particle networks with elastic moduli and yield strength one order of magnitude higher [32]. This is also observed in geological sediments.

There are two possible reasons for this puzzling observation. The different sol–gel kinetics might lead to different microstructures of the final gels, characterized by different coordination numbers of the particles in the network [48]. This was also found in computer simulations using Brownian dynamics

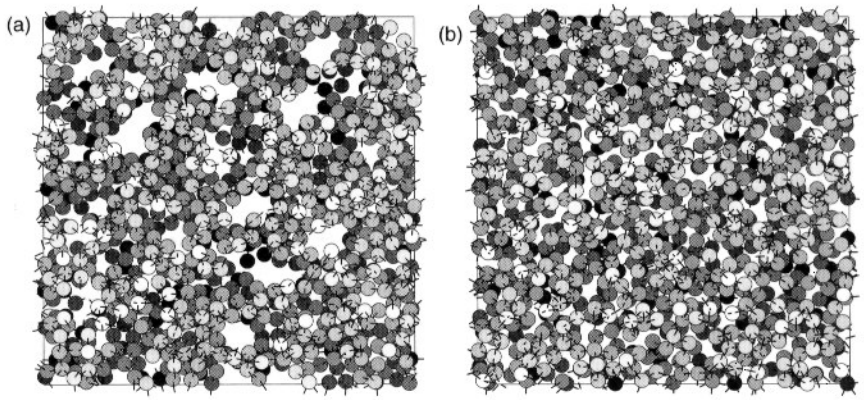

FIGURE 5.5.21 Simulated structures for 40 vol% coagulated particle suspensions (particles drawn in reduced size), from Ref. [41, p. 341]: (a) delayed coagulation due to energy barrier in interaction potential; rearrangement; (b) rapid switch from repulsive to purely attractive interaction potential, starting configuration is frozen in.

of monosized suspensions. Figure 5.5.21 illustrates the different microstructures resulting from different coagulation kinetics: on the one hand, a delayed coagulation due to an energy barrier in the interaction potential leads to a particle rearrangement (Figure 5.5.21a), on the other hand, a rapid switch from a repulsive to a purely attractive interaction potential preserves the random order of the particles (Figure 5.5.21b) [49]. Transferred to our system, case (a) can be seen as similar to the ΔI coagulation, case (b) as corresponding to ΔpH coagulation (see interparticle potential curves in Sections 5.5.3.1 and 5.5.3.2). The resulting local inhomogeneities in case (a) might strengthen the network, as discussed in Section 5.5.3.3.

Another possibility is that, due to the different chemical pathways, the bonds between the coagulated particles become different in strength. It is well known that the attractive interparticle potential in coagulated suspensions becomes much stronger upon decreasing the number of residual water layers between particles in contact [50]. It has recently been shown by new light scattering techniques such as diffusing wave spectroscopy that, after gelling, the microstructure of a polystyrene network remains unchanged whereas the dynamics show still considerable stiffening of the system during ageing [51]. This would support the hypothesis that, upon coagulating a suspension via increase of the ionic strength, the bonds between particles are strengthened with time.

A deeper insight into the structure and the mechanics of gel networks is yet to be acquired. Temperature-induced or enzymatically catalyzed internal

reactions, as outlined in this article, can essentially contribute to the clarification of such problems.

REFERENCES

1. Janney, M. A. (1990). Method for forming ceramic powder into complex shape. US Patent 4.894.194.
2. Young, A. C., Omatete, O. O., Janney, M. A., and Menchhofer, P. A. (1991). Gelcasting of Alumina. *J. Am. Ceram. Soc.* 74: 612–618.
3. Omatete, O. O., Strehlow, R. A., and Walls, C. A. (1992). Drying of gelcast ceramics. in *Ceramic Transactions, Vol. 26:* Forming Science and Technology for Ceramics, pp. 101–107, Cima M. J., ed., Westerville, OH: American Ceramic Society.
4. Sarkar, N., and Greminger Jr., G. K. (1983). Methylcellulose polymers as multifunctional processing aids in ceramics. *Am. Ceram. Soc. Bull.* **62**: 1280–1288.
5. Landham, R. R., Nahass, P., Leung, D. K., Ungureit, M., Rhine, W. E., Bowen, H. K., and Calvert, P. D. (1987). Potential use of polymerizable solvents and dispersants for tape casting of ceramics. *Am. Ceram. Soc. Bull.* **66**: 1513–1516.
6. Tormey, E. S., Pober, R. L., Bowen, H. K., and Calvert, P. D. (1984). Tape casting—future developments, in *Advances in Ceramics, Vol. 9: Forming of Ceramics*, pp. 140–149, Mangels J. A., and Messing G.L., eds., Columbus, OH: American Ceramic Society.
7. Cowan, R. E. (1976), in *Treatise on Materials Science and Technology, Vol. 9, Ceramic Fabrication Processes*, pp. 153–171, Wang F. F. Y., ed., New York: Academic Press.
8. Bollman, H. (1957). Unique new forming technique. *Ceram. Age*, **70**: 36–38.
9. Grala, E. M. (1957). Further investigation of the feasibility of the freeze casting method for forming fuel-size infiltrated titanium carbide turbine blades. NACA (Nat. Adv. Comm. Aeronaut.) Tech. Notes 3769; Ceram. Abstr., p. 108.
10. Maxwell, W. A., Gurnick, R. S., and Francisco, A. C. (1954). Preliminary investigation of the freeze casting method for forming refractory powders. NACA (Nat. Adv. Comm. Aeronaut.) Res. Memo E 53L21, p. 19.
11. Bergström, L. (1994). Method for forming ceramic powders by temperature induced flocculation, US Patent 5.340.532.
12. Napper, D.H. (1977). Steric stabilization. *J. Colloid Interface Sci.* **58**: 390–399.
13. Lange, F. F. (1986). Forming a ceramic by flocculation and centrifugal casting US Patent 4,626,808.
14. Velamakanni, B. V., Chang, J. C., Lange, F. F., and Pearson, D. S. (1990). New method for efficient colloidal particle packing via modulation of repulsive lubricating hydration forces. *Langmuir* **6**: 1323–1325.
15. Velamakanni, B. V., and Lange, F. F. (1993). Method for preparation of dense ceramic products, US Patent 5.188.780.
16. Franks, G. V., Velamakanni, B. V., and Lange, F. F. (1995). Vibraforming and in situ flocculation of consolidated, coagulated alumina slurries. *J. Am. Ceram. Soc.* **78**: 1324–1328.
17. Pujar, V. V., Cawley, J. D., Hu, P., and Lee, L. J. (1992). Reaction injection moulding of silica–alumina mixtures using heterocoagulation. *Mater Res. Soc. Symp. Proc.* **249**: 317–322.
18. Graule, T. J., Baader, F. H., and Gauckler, L. J. (1994). Shaping of ceramic green compacts direct from suspension by enzyme catalyzed reactions. *cfi/Ber. DKG* **71**: 317–323.
19. Graule, T. J., Baader, F. H., and Gauckler, L. J. (1994). Enzyme catalysis of ceramic forming. *J. Mater. Educ.* **16**: 243–267.

20. Graule, T. J., Baader, F. H., and Gauckler, L. J. (1995). Direct coagulation casting—a new green shaping technique, in *Ceramics: Charting the Future*, pp. 1601–1616, Vincenzini P., ed., Techna Srl.
21. Graule, T. J., Baader, F. H., and Gauckler, L. J. (1995). Casting uniform ceramics with direct coagulation. *Chemtech* **25**: 31–37.
22. Brinker, C. J., and Scherer, G. W. (1990). *Sol–Gel Science*, p. 240ff, New York: Academic Press.
23. Gauckler, L. J., Graule, T. J., and Baader, F. H. (1999). Ceramic forming using enzyme catalyzed reactions. *Mater. Chem. Phys.* **61**: 78–102.
24. Kistiakowsky, G. B., and Rosenberg, A. J. (1952). The kinetics of urea hydrolysis by urease. *J. Am. Chem. Soc.* **74**: 5020–5025.
25. Schmidt-Steffen, A. (1986). Untersuchung der Reaktion von Harnstoff mit an Membranen kovalent gebundener Urease (Investigation of the reaction of urea with urease bound covalently to membranes). PhD Thesis, Universität Essen.
26. Drauz, K., and Waldmann, H. (eds.) (1995). *Enzyme Catalysis in Organic Synthesis*, Vol. I, p. 113, Weinheim: VCH Verlagsgesellschaft mbH.
27. Rachhpal-Singh, and Nye, P. H. (1984). The effect of soil pH and high urea concentrations on urease activity in soil. *J. Soil Sci.* **35**: 519–527.
28. Grunwald, P. (1974). Physikalische und chemische Eigenschaften von freier und an aktivem Aluminiumoxid gebundener Urease (Physical and chemical properties of free urease and urease bound to active alumina). PhD Thesis, Universität Hamburg.
29. Balzer, B., Hruschka, M. K. M., and Gauckler, L. J. (2001). In-situ rheological investigation of the coagulation in aqueous alumina suspensions. *J. Am. Ceram. Soc.* **84**: 1733–1739.
30. Wyss, H. M., Romer, S., Scheffold, F., Schurtenberger, P., and Gauckler, L. J. (2001). Diffusing-wave spectroscopy in concentrated alumina suspensions during gelation. *J. Colloid Interface Sci.* **240**: 89–97.
31. Hidber, P. C., Graule, T. J., and Gauckler, L. J. (1996). Citric acid—a dispersant for aqueous alumina suspensions. *J. Am. Ceram. Soc.* **79**: 1857–1867.
32. Balzer, B., Hruschka, M. K. M., and Gauckler, L. J. (1999). Coagulation kinetics and mechanical behavior of wet alumina green bodies produced via DCC. *J. Colloid Interface Sci.* **216**: 379–386.
33. Yang, J., Huang, Y., Meier, L. P., Wyss, H. M., Tervoort, E., and Gauckler, L. J. (2002). Direct coagulation casting via increasing ionic strength. *Key Eng. Mater.* **224–226**: 631–636.
34. Wyss, H. M., Hütter, M., Müller, M., Meier, L. P., and Gauckler, L. J. (2002). Quantification of structure in stable and gelated suspensions from cryo-SEM. *J. Colloid Interface Sci.* **248**: 340–346.
35. Mueth, D. M., Jaeger, H. M., and Nagel, S. R. (1998). Force distribution in a granular medium. *Phys. Rev. E* **57**: 3164–3169.
36. Peterson, I. (1997). Dry sand, wet sand. Digging into the physics of sandpiles and sand castles. *Sci. News* **152**: 186–187.
37. Yanez, J. A., Laarz, E., and Bergström, L. (1999). Viscoelastic properties of particle gels. *J. Colloid Interface Sci.* **209**: 162–172.
38. Zallen, R. (1983). *The Physics of Amorphous Solids*, p. 170, New York, Wiley.
39. Yanez, J. A., Shikata, T., Lange, F. F., and Pearson, D. S. (1996). Shear modulus and yield stress measurements of attractive alumina particle networks in aqueous slurries. *J. Am. Ceram. Soc.* **79**: 2917–2924.
40. Channell, G. M., and Zukoski, C. F. (1997). Shear and compressive rheology of aggregated alumina suspensions. *AIChE J.* **43**: 1700–1708.
41. Hesselbarth, D., Tervoort, E. V., Urban, C., and Gauckler, L. J. (2001). Mechanical properties of coagulated wet Particle networks with alkali swellable thickeners. *J. Am. Ceram. Soc.* **84**: 1689–1695.

42. Gauckler, L. J., Si, W., Graule, T. J., Baader, F. H., and Will, J. (1999). Enzyme catalysis of ceramic forming: alumina and silicon carbide, in *Ceramics: Getting into the 2000's—Part C*, pp. 15–40, Vincenzini P., 9th Cimtec-World Ceramics Congress.
43. Si, W., Graule, T. J., Baader, F. H., and Gauckler, L. J. (1999). Direct coagulation casting of silicon carbide components. *J. Am. Ceram. Soc.* **82**: 1129–1136.
44. Hruschka, M. K. M., Si, W., Tosatti, S., Graule, T. J., and Gauckler, L. J. (1999). Processing of β-silicon nitride from water-based α-silicon nitride, alumina, and yttria powder suspensions. *J. Am. Ceram. Soc.* **82**: 2039–2043.
45. Baader, F. H., Will, J., Tièche, D., Graule, T. J., and Gauckler, L. J. (1995). High strength alumina produced by direct coagulation casting. *Ceramic Transactions*, Vol. 51, pp. 463–467. Ceramic Processing Science and Technology, The American Ceramic Society.
46. Katsuki, H., Kawahara, A., and Ichinose, H. (1992). Preparation and some properties of porous alumina ceramics obtained by the gelatination of ammonium alginate. *J. Mater. Sci.* **27**: 6067–6070.
47. Tervoort, E. V., private communication.
48. Hütter, M. (1999). Brownian dynamics simulation of stable and of coagulating colloids in aqueous suspensions, PhD Thesis, ETH Zürich.
49. Hütter, M. (2000). Local structure evolution in particle network formation studied by Brownian dynamics simulation. *J. Colloid Interface Sci.* **231**: 337–350.
50. Shih, W. Y., Shih, W.-H., and Aksay, I. A. (1999). Elastic and yield behavior of strongly flocculated colloids. *J. Am. Ceram. Soc.* **82**: 616–624.
51. Romer, S. (2001). Aggregation and gelation of concentrated colloidal suspensions, PhD Thesis, ETH Zürich.
52. Schönholzer, U. P., Hummel, R., and Gauckler, L. J. (2000). Microfabrication of ceramics by filling of photoresist molds. *Adv. Mater.* **12**: 1261–1263.